Towards a Videobronchoscopy Localization System from Airway Centre Tracking

Carles Sánchez[1], Antonio Esteban-Lansaque[1], Agnès Borrás[1], Marta Diez-Ferrer[2], Antoni Rosell[2]
and Debora Gil[1]

[1]*Computer Vision Center, Computer Science Department, UAB, Bellaterra, Spain*
[2]*Pneumology Unit, Hospital Universitari Bellvitge, IDIBELL, CIBERES, Barcelona, Spain*

Keywords: Video-bronchoscopy, Lung Cancer Diagnosis, Airway Lumen Detection, Region Tracking, Guided Bronchoscopy Navigation.

Abstract: Bronchoscopists use fluoroscopy to guide flexible bronchoscopy to the lesion to be biopsied without any kind of incision. Being fluoroscopy an imaging technique based on X-rays, the risk of developmental problems and cancer is increased in those subjects exposed to its application, so minimizing radiation is crucial. Alternative guiding systems such as electromagnetic navigation require specific equipment, increase the cost of the clinical procedure and still require fluoroscopy. In this paper we propose an image based guiding system based on the extraction of airway centres from intra-operative videos. Such anatomical landmarks are matched to the airway centreline extracted from a pre-planned CT to indicate the best path to the nodule. We present a feasibility study of our navigation system using simulated bronchoscopic videos and a multi-expert validation of landmarks extraction in 3 intra-operative ultrathin explorations.

1 INTRODUCTION

Lung cancer is one of the most incidental neoplasms in Europe with around $437,773$ new cases estimated for 2015 [1]. Screening programs increase lung cancer early diagnosis and, thus, may significantly reduce the risk of death (Aberle et al., 2011). Screening programs are based on the detection of small pulmonary lesions with low dose chest computed tomography (CT) and its pathological confirmation. Pathological confirmation requires either transthoracic needle aspiration or an endoscopic examination. Transthoracic needle aspiration has some complications (Manhire et al., 2003), like pneumothorax (20%). Conventional bronchoscopic diagnostic procedures are visually guided using radiating fluoroscopy and render a suboptimal 34% of positive results for lesions < 2 cm (Donnelly and Edwin, 2012). New endoscopy techniques (like virtual bronchoscopy or electromagnetic techniques) are expensive, require either manual intervention or special gadgets, only increase diagnostic yield to 70% (Aberle et al., 2011), and still radiate the patient. The 30% undiagnosed pulmonary lesions need CT follow-up or futile surgery procedures such

as thoracoscopies (Aberle et al., 2011). Diagnostic yield could be improved reducing radiation and costs if imaging technology could better detect and guide the bronchoscopist to the target lesion.

A main limitation of flexible bronchoscopy is the difficulty to determine the correct pathway to peripherial lesions. CT Virtual Bronchoscopy (VB) can precede bronchoscopy to assess the optimal path using virtual navigation. VB is a computer simulation of the video bronchoscope image from the bronchoscope camera (Reynisson et al., 2014) which is created from the 3D CT volume, with the same view angle and zoom settings. Despite different approaches to VB, existing systems fail due to several aspects at planning and exploration time.

During exploration, VBs should accurately guide the operator across the planned path to the biopsy point. Standard protocols relying on fluoroscopy have a diagnostic yield around 40%, last 20 min per intervention and require 5-10 min of repetitive patient and medical staff radiation (Asano et al., 2013). Existing alternatives like image based systems (LungPoint, NAVI) or electromagnetic navigation (inReachTM,SPinDriveA) are far from meeting clinician expectations. Image systems are based on multimodal registration of CT virtual projections to bron-

---

[1]globocan.iarc.fr

choscopy frames and require manual intra-operative adjustments of the guidance system (Eberhardt et al., 2010). Electromagnetic systems require specific gadgets (Gildea et al., 2006), that alter the operating protocol and increase intervention cost.

The potential of image processing in enhancing guiding capabilities has not been fully explored. To display the correct position of the bronchoscope in the CT-derived maps (structural maps of airways), scope position should be tracked in videos. Some solutions consist in hybrid algorithms (Luó et al., 2012) (feature tracking and multimodal registration) but most of current solutions are based on multimodal registration (Reynisson et al., 2014) of CT virtual projections to the actual videobronchosocpy frame (Mirota et al., 2011). A main disadvantage is that the view from the bronchoscope can be obscured by blood or mucus, causing the tracking between video images and CT to be disrupted. Another flaw is the sensitivity to common sudden changes in image appearance and camera motion.

An alternative to image registration is the use of anatomical landmarks representing airway geometry to match CT planning to current navigation path. Some authors (Hofstad et al., 2015) use airways centreline extracted using an electromagnetic tracking sensor on the tip of the bronchoscope. Another option is to extract landmarks representing the intrinsic local geometry of airways which allows its identification in, both, CT scans and videos without any extra device (Sánchez et al., 2015b). Such geometric features can be encoded using a computational data structure for path matching. Landmark extraction in interventional videos is challenging due to the large variety of image and motion artefacts and the unpredicted presence of endoscopic devices. Although recent works (Sánchez et al., 2014; Sánchez et al., 2015a) have developed reliable processing methods to extract endoluminal structures, they are designed for 2D image analysis and might fail applied to videos.

We propose a codification of airways as a binary tree defined by bronchial branches to match lumen centres between CT and videobronchoscopy. Lumen centres are tracked in images using a multiscale approach based on maximally stable external regions (MSER) (Matas et al., 2004). Tracked centres together with detection of branching points are used to match the VB planing and the current exploration. The feasibility of our landmark based CT-Video matching is tested on several video sequences simulated on a VB interface platform. The capability for intra-operative matching is checked by assessing the quality of the tracked centres in ultrathin real explorations. These first results show the potential of

our methodology to accurately reach most distal levels in ultrathin navigation.

2 CT-VIDEO ANATOMICAL MATCHING

The bronchial tree has a tubular geometry and, thus, it is described as far as its central line (airway lumen centre) and walls (luminal area) are extracted. In the case of bronchial navigation, the path can be described using the lumen centre position and the branching points of the bronchial tree structure.

Our CT-video path matching locates the current position of the scope by comparing the bronchial tree extracted from the CT used to plan the intervention to a bronchial structure generated from the tracking of lumen centres extracted from videobronchoscopic images during intervention time. Both anatomical structures can be computationally encoded by means of a binary tree (Sánchez et al., 2015b) with nodes given by the bronchial branching levels. The matching between CT-video bronchial structures is then given by comparing the two binary trees.

2.1 Bronchial Anatomy Encoding from the CT Scan

The whole bronchial tree to be matched to the current exploration navigation path is encoded from the skeleton of a segmentation of the CT volume. The skeleton is obtained using (Van Uitert and Bitter, 2007) with a branch pruning based on its length. The 3D binary volume containing the one-dimensional voxel skeleton is converted (Kerschnitzki and et al., 2013) into a network graph described by nodes (skeleton branching points) and edges (branch joining two nodes) or equivalently by the adjacency matrix.

The skeleton adjacency matrix is a symmetric matrix with non-zero entries whenever two nodes are connected by an edge and, thus, it codifies an undirected graph with the 1st node at the trachea. The graph is traversed to obtain the binary tree that encodes airways anatomy. Each node is visited by iteratively traversing the graph starting from the 1st node to create a list of all the visited nodes. This list correspond to all parents the node is connected to and it is used to remove edges from the adjacency matrix to get the tree structure.

The final binary tree is defined by labelling each branch according to its bronchial level and orientation (left, right) with respect the splitting branch at the previous level. The tree top node corresponds
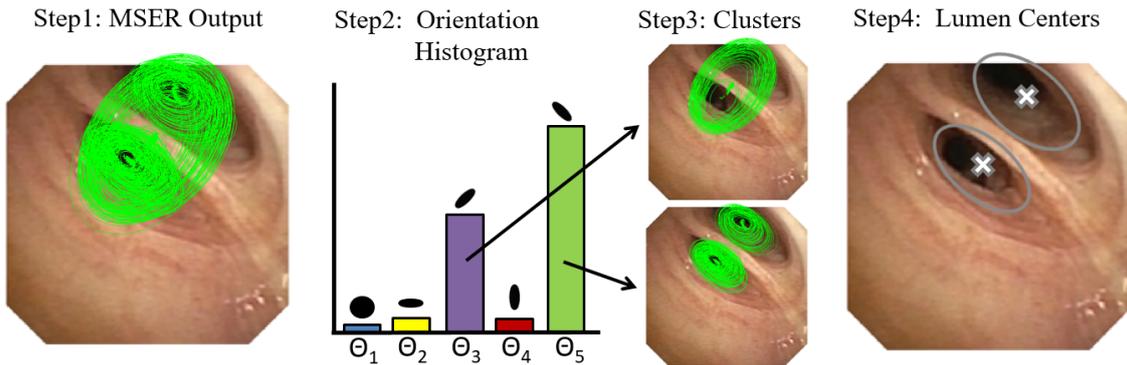
Figure 1: Extraction of Lumen Centres using a Multi-scale MSER.

to the tracheal entry point and it is labelled "0". At each new branch, the added nodes are labelled "0" or "1" depending on the anatomical branch orientation ("0" for left, "1" for right). To label branches at each level, we use the orientation of the current and children nodes with respect to the current node parent. Let $P_n = (x_n, y_n, z_n)$, $P_p = (x_p, y_p, z_p)$ and $P_{ch_i} = (x_{ch_i}, y_{ch_i}, z_{ch_i})$ be the 3D positions in the airway skeleton of the current node, n, its parent, p, and current node children, ch_i, $i = 1, 2$. Taking P_n as origin of coordinates, such positions define a coordinate change in $\mathcal{R}^3$ given by the vectors $\overrightarrow{V}_0 = P_p - P_n$, $\overrightarrow{V}_1 = P_{ch_1} - P_n$ and $\overrightarrow{V}_2 = P_{ch_2} - P_n$. Each children node n_{ch_i} is labelled "0" or "1" depending on the orientation (clock wise or counter clock wise) of the basis given by $\overrightarrow{V}_0$, $\overrightarrow{V}_1$, $\overrightarrow{V}_2$. Since the orientation of a coordinate change is determined by the sign of the determinant of the matrix given by the vector coordinates, children nodes are labelled according to:

$$Label(ch_1) = \begin{cases} 0 & \text{, if } det((\overrightarrow{V}_0, \overrightarrow{V}_1, \overrightarrow{V}_2)) > 0 \\ 1 & \text{, otherwise} \end{cases}$$
$$Label(ch_2) = 1 - Label(ch_1) \qquad (1)$$

for $(\overrightarrow{V}_0, \overrightarrow{V}_1, \overrightarrow{V}_2)$ the matrix given by the column vectors $\overrightarrow{V}_i$, $i = 1, 2, 3$.

2.2 Bronchial Path from Exploration Videos

The computation of the navigated path has 2 stages: extraction of lumen centres in images using a multi-scale MSER over a likelihood map of lumen centre location and tracking of MSER centres to endow continuity across the sequence.

Extraction of airway centres is based on likelihood maps (Sánchez et al., 2014) with maximum values at candidate centres. Under the assumption of a circular luminal profile in central navigation, such maps use a

single scale isotropic Gaussian kernel to characterize dark image areas prone to belong to airway lumen. Unlike (Sánchez et al., 2014), we compute several maps using a bank of anisotropic Gaussian filters with different orientations and scales to model non-circular lateral bronchi and small distal levels. Gaussian filters have been normalized by their L^2 norm to obtain more uniform responses comparable across different scales and degrees of anisotropy.

To compute local maxima consistent across scales and orientations, we use maximal stable extremal regions (MSER) in the multi-scale scheme sketched in fig.1. A set of MSER elliptical regions are extracted for each likelihood map (fig.1, step1). To endow stability across likelihood maps and, thus, different scales and orientations, MSER regions are first split according to their orientation using a histogram (fig.1, step2). For each orientation, elliptical MSER regions are sorted by their area and grouped into N clusters (fig.1, step3). The union of all ellipses in each cluster defines a set of N regions that are filtered using an inclusion criteria. The overlapping between regions is computed and those having maximum overlap are selected. The collection of MSER centroids for all valid regions are the set of lumen centres for each frame (fig.1, step4).

To endow centres with temporal continuity, MSER candidates are tracked using a modified Kalman filter (Haykin, 2004). For each lumen centre at a given frame, a Kalman filter (Haykin, 2004) predicts its location in the next frame according to a motion model (constant velocity, constant acceleration). Such motion models are prone to fail in intra-operative videos due to abrupt movements in scope manual guiding and patient coughing. To reduce the impact of these variations in motion model, we have implemented a constant position tracker that uses a state vector with zero velocity.

2.3 CT-Navigation Matching

To match the navigation path to the binary tree encoding CT bronchial anatomy, we identify frames traversing a higher bronchial level (binary tree level) and orient the entering branches to chose the tree node. A given frame at time, t, can be categorized from the multiplicity of lumen centres, NLM, as: 1) Frame within same bronchial level ($NLM_{t+1} = NLM_t$); 2) Frame approaching a bronchial level ($NLM_{t+1} > NLM_t$); 3) Frame traversing a bronchial level ($NLM_{t+1} < NLM_t$). Starting at the top node of the binary tree, each time a frame traverses a bronchial level, the tree level is increased and the path node sequence is updated by adding "1" or "0" depending on the entering branch orientation. The centre point with highest likelihood is considered to be the scope current position and defines the entering branch. Its orientation is defined by its relative position with respect the disappearing centres. If the x-coordinate is larger than the average x-coordinate of the vanishing points, we consider that the node is labelled "1" and "0" otherwise.

Figure 2 illustrates the main steps involved in our CT-video matching based on the codification of airways anatomical landmarks. We show the skeleton of a segmented CT scan (left image) that represents the centre airway line and the final binary tree data structure for the first 3 bronchial levels (central image). We have labelled the skeleton branching points according to their corresponding binary tree nodes, so that the green path would correspond to the node sequence $(1, 0, 1, 0)$. The most right images illustrate the identification of lumen centres and the matching to the binary tree (central image) representing the exploration bronchial path. Lumen centres in right images are plotted in green, with dots indicating the one corresponding to the scope current position. We show two representative cases: a frame within same bronchial level (top images) and a traversing frame (bottom images). The node sequence associated to these frames is shown on the central tree in green.

3 EXPERIMENTS

3.1 Experiment1: Tracked Centres Accuracy

We have compared under intervention conditions the quality of centres tracked using Section 2.2 (labelled MSER) to the method in (Sánchez et al., 2015b) exclusively based on local maxima (labelled

LMx). Methods have been applied to 3 ultrathin bronchoscopy videos performed for the study of peripheral pulmonary nodules at Hospital de Bellvitge. Videos were acquired using an Olympus Exera III HD Ultrathin videobronchoscope. For each video, we considered one proximal (up to 6th division) and one distal (above 6th) fragments. The maximum bronchial level achieved in our ultrathin explorations was within 10th and 12th, which is in the range of the maximum expected level reachable by ultrathin navigation (Asano et al., 2013). Fragments included the most common artefacts of intra-operative videos: bronchoscope collision with the bronchial wall, bubbles due to the anaesthesia and patient coughing.

For each fragment, we sampled 10 consecutive frames every 50 frames. Such frames were annotated by 2 clinical experts to set false detections and the position of missed centres. Inspired in crowd sourcing strategies (Maier-Hein et al., 2015), annotations were blended to get a unique ground truth using the intersection of the two annotated point sets as illustrated in fig.3. Ground truth sets were used to compute precision (Prec) and recall (Rec) for each set of consecutive frames. These scores are taken for all such sets in distal and proximal fragments for statistical analysis. We have used a T-test for paired data to assess significant differences across methods average precision and recall and confidence intervals, CI, to report average expected ranges. Tests and CIs have been computed at significant level $\alpha = 0.05$.

Table 1 reports CIs for each score and method at proximal and distal levels, as well as, p-values for the difference between MSER and LMx scores. At proximal level, both methods perform equally, but MSER keeps its quality scores at distal levels. This introduces significant differences (p-val< 0.05) in distal and total Prec and Rec. Such differences are larger for Rec, with a CI for the difference equal to $[0.05, 0.16]$ for distal bronchi and $[0.03, 0.16]$ overall. It is worth noticing that the proposed method always has a 100% of precision and a recall over 86%, with non-significant differences between distal and proximal levels (p-val > 0.7).

To validate the stability of our tracked centres in full explorations, we have applied our MSER tracking to one of the complete videos. The chosen video starts at carina, reaches the 11th level and includes back and forth navigation with bronchoscope rotation. Concerning image quality, there are saturation illumination artefacts at most distal levels and some fragments were recorded using narrow band imaging. The original video with the tracked centres on each image frame with a colour legend indicating candidate centres discarded by the Kalman filter, tracked
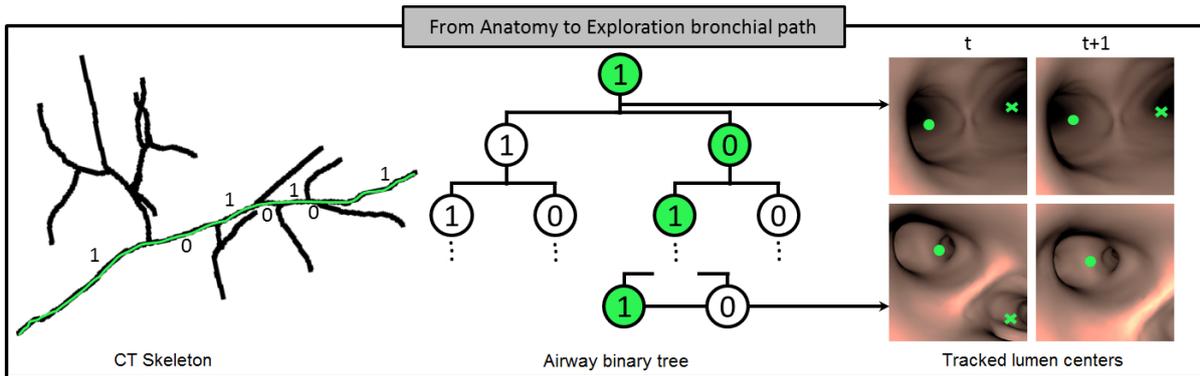
Figure 2: CT-Video Anatomical Matching. Codification of the bronchial anatomy from CT branch points (right image) and binary tree coding for identification of the navigated path inside the bronchial tree (central and left images).
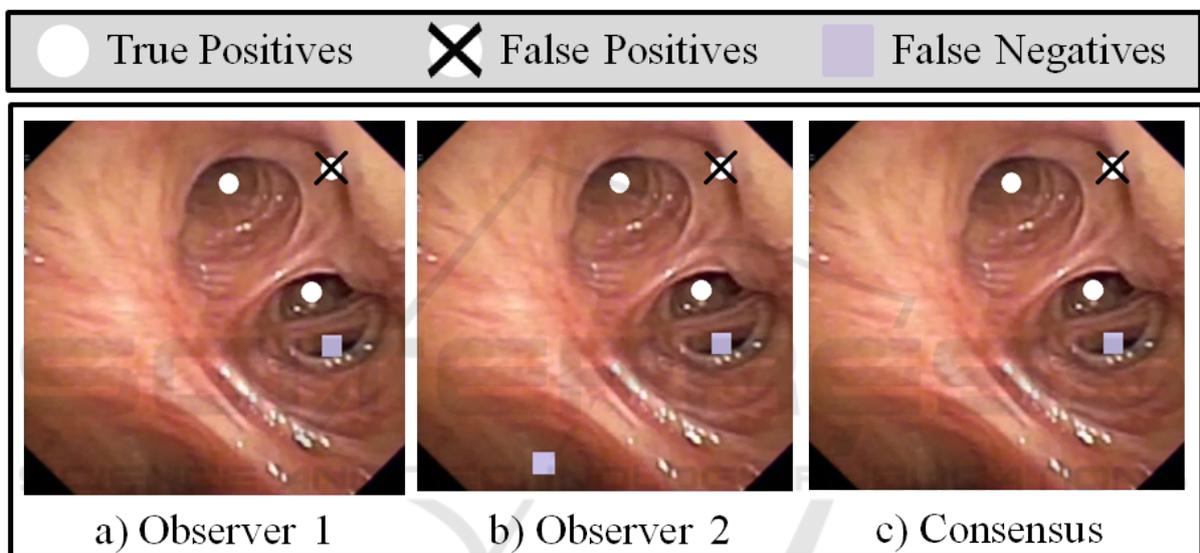
Figure 3: Manual Annotation of Tracked Centres.

Table 1: Average precision and recall confidence intervals for centre tracking.

	Proximal			Distal		
	MSER	LMx	p-val	MSER	LMx	p-val
Prec	$[1.0, 1.0]$	$[0.95, 1.0]$	0.07	$[1.0, 1.0]$	$[0.93, 0.99]$	0.02
Rec	$[0.86, 1.0]$	$[0.81, 0.96]$	0.4	$[0.82, 0.97]$	$[0.74, 0.87]$	$7e-4$

centres and scope position is available at https://www.youtube.com/watch?v=h8kUrzDjSKo. Figure 4 shows representative frames at proximal (a,b) and distal (c,d) levels.

3.2 Experiment2: Anatomical Matching Accuracy

We have tested our methodology in virtual explorations of CT volumes from 3 patients coming from Hospital de Bellvitge. CT scans were acquired with a 320-detector row Aquilion ONE, Toshiba CT scan and 0.5 mm thickness. Each CT volume was manually segmented using AMIRA to create a triangular mesh in .obj format for navigation simulation. Virtual explorations were generated using a simulation platform developed in Unity (Borras et al., 2015), which allows the modelling of the scope camera and interactive point of view navigation. For this experiment, the bronchoscope was simulated in central navigation without rotation around the scope long axis (see the Discussion Section 4 for clarifications about this assumption). The camera position inside the bronchial
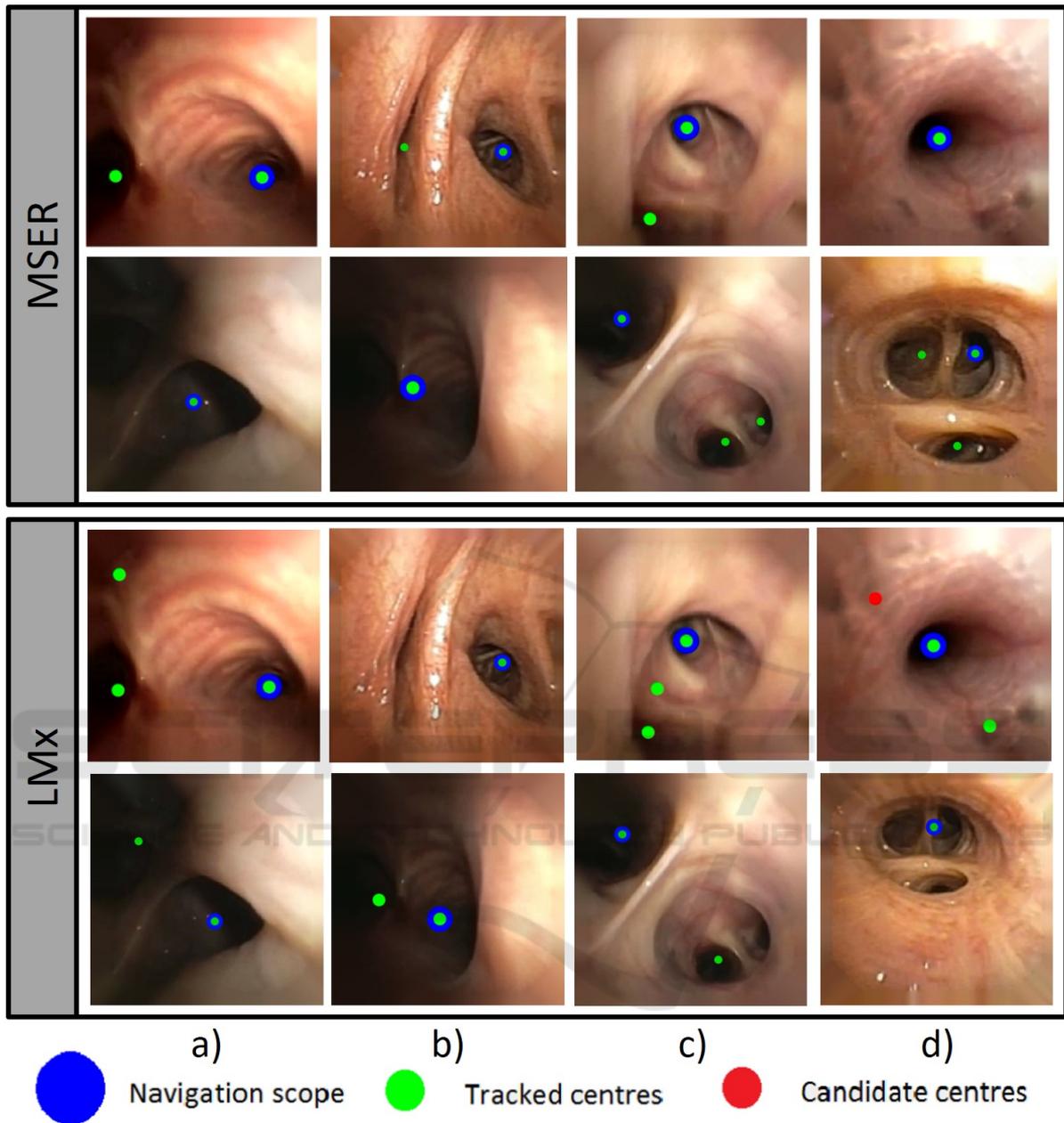
Figure 4: Representative frames at proximal, (a,b) and distal levels, (c,d).

tree was exported to define the codification of the ground truth path in the binary tree.

For each CT scan, 15 virtual explorations with different branching paths and bronchial levels (from 4th to 12th) were defined. For each path, the binary tree node coding for the ground truth camera position was compared to the code extracted from virtual videos. Node path coding was compared in terms of True Positives Nodes (TPN) and True Path Representations (TPR). For a given exploration, a node is con-

sidered to be a TPN if its label coincides with the GT node label. The number of consecutive TPN achieved from the 1st node divided by the path node length defines TPR. As before, we have used a T-test to detect significant differences across proximal and distal levels and CIs at significance $\alpha = 0.05$ to report average TPN and TPR.

Table 2 reports CIs for average TPN, TPR percentages at proximal and distal levels and p-values of the T-test for the difference. The detection rate of

Table 2: Comparison of TPN and TPR at proximal and distal levels.

	Proximal	Distal	p-val
TPN	$[70.32\%, 85.86\%]$	$[67.32\%, 81.18\%]$	0.4397
TPR	$[72.16\%, 90.71\%]$	$[63.91\%, 79.53\%]$	0.0370

nodes along the whole path is not significantly different at distal and proximal levels, with a CI for the difference equal to $[-6.1\%, 13.8\%]$. Concerning the percentage of correct paths reached from the trachea, there are significant differences with a drop between $[1.3\%, 15.9\%]$. This drop in performance mainly arises from false distal centres due to illumination artefacts in simulated data and a suboptimal labelling of CTs (see Discussion Section 4 for details).

4 DISCUSSION AND CONCLUSIONS

We have introduced a localization system for lung cancer biopsy guidance based on identification of airways centres. The system bases on a codification of airways using a binary tree and an airway lumen extraction from videobronchoscopy with an ultrathin bronchoscope. Our experiments validate centre extraction in 3 intra-operative ultrathin videos and the CT-video path retrieval in simulated data.

Results in ultrathin bronchoscopy videos indicate high equal performance of our centre tracker based on maximal stable regions at proximal and distal levels. In particular, there are not any false detections (Prec=1) and the rate of missed centres is under 15% (Rec> 0.85). The decrease in recall is due to the model assumptions used to compute the likelihood maps (Sánchez et al., 2014), which even using anisotropic Gaussians favour circular geometries. This could be solved by considering the bronchial structure of each patient extracted from the CT-scan. This expected local configuration of airway centres could be used during the tracking step to retrieve missing lateral bronchi. Still, results are promising enough (see the full exploration at `https://www.youtube.com/watch?v=h8kUrzDjSKo`) to encourage a use in a navigation system to explore the benefits of using video information for biopsy guidance to peripheral pulmonary nodules.

The potential of our centre tracking for CT-navigation matching is illustrated in the experiment with simulated data. It is worth noticing that the quality of tracked centres is enough to correctly match 80% of 6th level paths and 70% of 12th level paths using only multiplicity of the tracked centres. Of course this matching criteria is not powerful enough to cope

with artefacts in centres detection, which introduce false nodes in the tree path coding for distal paths. We think that codification of the full MSER regions hierarchy would provide a more solid representation of bronchial branching in images and,thus, increase the level successfully matched. Aside, the labelling of the CT tree should take into account the local orientation (Frenet basis) of the path traversing bronchial level to obtain a labelling consistent with image projection orientation. Finally, simulations were done assuming central non-rotational navigation. This is not a critical assumption, provided that the goal was to validate a CT-video matching based on lumen anatomical landmarks as alternative to image registration. However, to have a system operative in clinical conditions, the criteria used to label image centre lumens should be modified to allow rotations of the bronchoscope. This could be achieved by computing the intra-frame rotation to adapt the position of centres in central navigation to the current exploration and it is future work.

ACKNOWLEDGMENTS

REFERENCES

Aberle, D., Adams, A., and et. al. (2011). Reduced lung-cancer mortality with low-dose computed tomographic screening. *N Engl J Med*, 365:395–409.

Asano, F., Shinagawa, N., and et. al. (2013). Virtual bronchoscopic navigation combined with ultrathin bronchoscopy. arandomized clinical trial. *AJRCCM*, 188(3):327–333.

Borras, A., Gil, D., and et al. (2015). A virtual bronchoscopic tool to explore the impact of physical restrictionsin bronchoscopy planning. In *MICCAI IMIM*.

Donnelly, E. and Edwin, F. (2012). Technical parameters and interpretive issues in screening computed tomographyscans for lung cancer. *JTI*, 27(4):224–229.

Eberhardt, R., Kahn, N., and et. al. (2010). Lungpointa new approach to peripheral lesions. *JTO*, 5(10):1559–1563.

Gildea, T., Mazzone, P., and et. al. (2006). Electromagnetic navigation diagnostic bronchoscopy: a prospective study. *AJRCCM*, 174(9):982–989.

Haykin, S. (2004). *Kalman filtering and neural networks*, volume 47. John Wiley & Sons.

Hofstad, E., Sorger, H., and et. at (2015). Automatic registration of ct images to patient during bronchoscopy- a clinicalpilot study. In *ECBIP*.

Kerschnitzki, K. and et al. (2013). Architecture of the osteocyte network correlates with bone material quality. *JBMR*, 28(8):1837–45.

Luó, X., Feuerstein, M., and et al (2012). Development and comparison of new hybrid motion tracking for bronchoscopicnavigation. *Medical image analysis*, 16(3):577–596.

Maier-Hein, L., Kondermann, D., and et. al. (2015). Crowdtruth validation: a new paradigm for validating algorithms that relyon image correspondences. *IJCARS*, 10(8):1201–12.

Manhire, A., Charig, M., and et. al. (2003). Guidelines for radiologically guided lung biopsy. *Thorax*, 58(11):920.

Matas, J., Chum, O., Urban, M., and Pajdla, T. (2004). Robust wide-baseline stereo from maximally stable extremal regions. *IMAVIS*, 22(10):761–767.

Mirota, D., Ishii, M., and Hager, G. (2011). Vision-based navigation in image-guided interventions. *Annual review of biomedical engineering*, 13:297–319.

Reynisson, P., Leira, H., and et. al (2014). Navigated bronchoscopy: a technical review. *JBIP*, 21(3):242–264.

Sánchez, C., Bernal, J., and et al (2014). On-line lumen centre detection in gastrointestinal and respiratory endoscopy. In *MICCAI-CLIP*, volume 8361 of *LNCS*, pages 31–38.

Sánchez, C., Bernal, J., Sánchez, F. J., Diez, Marta andRosell, A., and Gil, D. (2015a). Toward online quantification of tracheal stenosis from videobronchoscopy. *IJCARS*, 10(6):935–945.

Sánchez, C., Gil, D., and et al (2015b). Navigation path retrieval from videobronchoscopy using bronchial branches. In *CLIP, LNCS 9401*.

Van Uitert, R. and Bitter, I. (2007). Subvoxel precise skeletons of volumetric data based on fast marching methods. *Medical physics*, 34(2):627–638.